

## ON THE TENSION FIELD ACTION AND COLLAPSE MECHANISM OF A PANEL UNDER SHEAR

*By Shigeru KURANISHI\*, Masatoshi NAKAZAWA\*\* and Tetsuo IWAKUMA\*\*\**

The development of the tension field and the collapse mechanism of shear panels isolated from plate girders are numerically investigated by the finite element method. Special attention is paid to the influence of the rigidity of flanges and the boundary conditions of one panel. It is then recognized that no plastic hinge appears in flanges even in the ultimate state, and that a collapse mechanism is formed when the yielded zones propagate completely in the diagonal direction of the panel. Furthermore, discussed are the relationships between the configuration of the tension field or the inclination of the tensile principal stress and the anchor action by the sided members or the gusset plate action.

*Keywords: plate girder, shear, tension field, collapse mechanism, FEM*

### 1. INTRODUCTION

Thin plated structures are generally designed in expectation of the post-buckling strength of their component plates. Especially, it is well known that the tension field produced in the end panels of plate girders gives a relatively large amount of additional load carrying capacity even after buckling of web plates in shear. Therefore, many researchers have conducted the experimental and theoretical studies about the relationship between the shear strength and this tension field action, and their results have been introduced in provisions of the structural design codes in several countries. However, there are still proposed a number of new ideas and theories about this subject, and a widely accepted theory and the corresponding design formula have not been established yet. For example, in the Japanese Specifications for Highway Bridges<sup>1)</sup>, the effect of the additional post-buckling strength is taken into account simply by the reduction of the factor of safety.

In the experimental approach, it is very difficult to simulate the actual behavior of end shear panels in the plate girders. Also the differences in the experimental models tested with different loading conditions and structural parameters lead to a variety of collapse mechanism models and many different conclusions. Generally, the strength and deformation of a shear panel are influenced not only by the geometrical parameters of a web but also by the mechanical characteristics of flanges and transverse stiffeners and the boundary conditions. Even with the transverse stiffeners rigid enough to make the adjoining panels behave independently at buckling, the collapse mechanism may depend on the contribution of flanges to the tension field. There exist two basic models of the collapse mechanism, one of which is proposed by Basler<sup>2)</sup>, and

\* Member of JSCE, Dr. Eng., Professor, Department of Civil Engineering, Tohoku University (Aoba Sendai 980 JAPAN)

\*\* Member of JSCE, M. Eng., Research Associate, Department of Civil Engineering, Tohoku University

\*\*\* Member of JSCE, Ph. D., Associate Professor, Department of Civil Engineering, Tohoku University

another by Cardiff-University-Group represented by Rockey<sup>3)~5)</sup>. Basler included the so-called anchor action by the transverse stiffeners and the neighboring panels, but not by the flanges. Consequently, the deformed configuration of a rectangular panel is parallelogrammatic, and the shear panel achieves its ultimate state when the full yielding is developed in the tension field band. On the other hand, Cardiff-University-Group observed the anchor action by flanges in their experiments, and presented a new collapse model. They assume that the resistance of a panel is lost when the skew tensile stress in the tension field bends flanges to form plastic hinges in them. The width of the tension field is then governed by the location of the plastic hinges. Namely, their final deformed configuration of the panel is that the upper and lower triangular parts and the tension field band slide each other in the opposite directions; see Fig. 10 (b). Fujii<sup>6)</sup> assumed a similar collapse mechanism model with the plastic hinges located always at the center of the flanges. Komatsu<sup>7)</sup> and Herzog<sup>8)</sup> also presented independently their original collapse mechanism models with plastic hinges, and the location of which depends on the rigidity of the flange.

Recently, the numerical analysis of these problems becomes feasible because of the development of large computers and the advances in the structural analysis. However, the analyses of the tension field and the ultimate shear strength are still very difficult because of the requirements of complicated but precise calculations with both geometrical and material nonlinearity. Very few studies<sup>9)~11)</sup> concerning to these problems have been conducted, but only a plate rather than a panel isolated from a plate girder has been examined. In the numerical approach, there also exist the similar problems to those in the experimental study; e. g. how to specify the boundary conditions of a panel isolated from a structure. In this paper, the shear strength of a panel is analyzed numerically with emphasis on the influence of the boundary condition which includes the effect of the sided members. The anchor action by the sided members and the development of the tension field are discussed by varying the degrees of constraints on the boundaries and tracing the behavior of a shear panel. Finally, the collapse mechanism and the characteristics of the shear strength are presented, and the results are compared with the available experimental ones<sup>2)~5)</sup>.

## 2. METHOD OF ANALYSIS AND MODELS

### (1) Method of analysis

The panel isolated from a plate girder is a spatial structure which consists of a web plate and flange plates connected perpendicular to each other. However, most plate finite elements in general use neglect the in-plane rotational freedom at their nodes, so that the compatibility condition along the joint line is not satisfied when two elements are connected inclined to each other. Therefore, the calculated stresses may not be reliable. For more accurate analysis, the triangular element with 6 degrees of freedom per node is used in order to connect the adjoining elements rationally, and the hybrid method by an assumed stress distribution<sup>12)~15)</sup> is employed here. A linearized local stiffness equation is derived for the small incremental displacements. A nonlinear global equilibrium equation of incremental form is then solved by the successive approximation until a sufficient convergence is obtained. For isotropic steel materials, Young's modulus  $E$ , the shear modulus  $G$ , Poisson's ratio  $\nu$  and the tensile yield stress  $\sigma_y$  are set 206 GN/m<sup>2</sup>, 79 GN/m<sup>2</sup>, 0.3 and 235 MN/m<sup>2</sup> respectively. The effective stress-strain relationship is assumed to be bilinear with strain-hardening, the rate of which is set  $E/1000$ . Only the kinematic hardening effect with the rule by Ziegler<sup>16)</sup> is taken into account. The associated flow rule is employed in the incremental plastic stress-strain relationship. Each plate element has 8 layers to consider the development of yielded zones in the plate thickness direction. The stiffness of a whole plate element in the elastic-plastic range is then evaluated numerically by adding up the stiffness contribution of each layer<sup>17)</sup>. The web and flange plate are divided into  $10 \times 10$  and  $2 \times 10$  meshes respectively with accuracy check by the convergence study, to make the total numbers of triangular elements 280 as shown in Fig. 1. It has been checked that the divided number of the flange plate does not affect the behavior and strength of the web panel, and present meshes are enough for the analyses below. The initial out-of-plane deflection  $W_0$  of a

web plate is given by the doubly sinusoidal half wave, and its central deflection is  $1/250$  of the panel depth. The introduction of the magnitude of this imperfection is based on the tolerance limit in the regulation of the Japanese Specification for Highway Bridges<sup>1)</sup>. However, as Moriwaki and Fujino<sup>18)</sup> reported, the initial deflections and the distribution of residual stress in web plates do not have so much influence on the ultimate shear strength. Because a web plate has the relatively high post-buckling strength and shows the large deformations compared with the initial ones. Therefore, throughout this analysis, the residual stresses are neglected, but the initial deflections are taken into account to analyze the post-buckling behavior more easily and their magnitude and shape are fixed in all cases. The structural parameters used in this numerical analysis are as follows; aspect ratio of a web plate  $\alpha=0.5, 0.75, 1.0$  and  $1.5$ ; width-thickness ratio of a web plate  $\beta=152, 180$  and  $250$ .

In order to exaggerate the influence of flange rigidity on the deformation and ultimate shear strength, the flange with reduced rigidity from the standard one defined in the Appendix is used. The reduction ratio of the torsional rigidity  $\gamma_t$  and of the lateral flexural rigidity  $\gamma_l$  are set  $1/3$  or  $1/5$  when necessary, but are usually  $1.0$ .

## (2) Modeling of a panel

When a panel is isolated from a whole structure for the analysis, it becomes very difficult to give the boundary conditions to simulate the actual behavior of the panel appropriately. In this study, three boundary conditions are considered in order to check their effects. Fig. 2 shows these models with different boundary conditions. Although the model I and II have flanges on their upper and lower edges, the model III does not. In all cases, the side edges are simply supported; i.e. the out-of-plane displacement is kept zero there.

The boundary condition of model I shown in Fig. 2(a) severely restricts the deformation of a panel most among these cases, because the in-plane longitudinal displacement is fixed along both sides. This model simulates the panel with the adjoining panels attached on both sides, and thus the direct anchor action by these sided members as well as flanges can be included. The bending moment varies linearly and is zero on the center line of the panel. In model II in Fig. 2(b), the in-plane displacement is free along the right-hand side edge. The bending moment is zero there and can take the value of the applied bending moment at the left-hand side edge. Therefore in this case, the direct anchor action by the sided members included in model I is presumably excluded on the right edge, and the shear strength may be lower than that of model I. In model III in Fig. 2(c), all four edges are simply supported and are subjected to pure shear loading. The in-plane longitudinal displacement, however, is fixed on both side edges. Therefore, the direct anchor action by the sided members can be expected, but that by flanges can not be included. In actual plate girders, this pure shear state in the end panel does not occur, but it should be worth checking the pure shear strength characteristics of panels without the effect of bending moment or the rigidity of

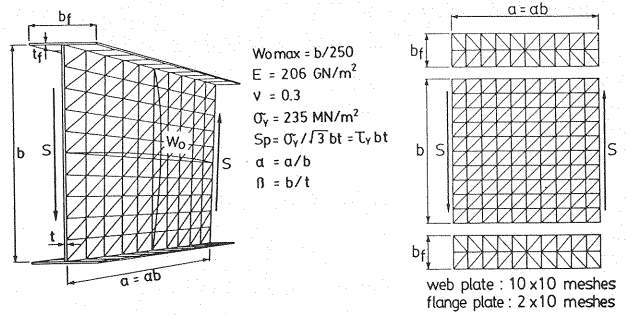


Fig. 1 Model for the numerical analysis.

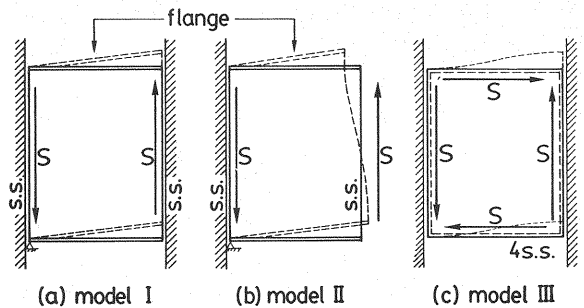


Fig. 2 Models with various boundary condition; S is shear force.

flanges for comparison.

One of the sequential panels taken out here is assumed to be subjected to the same loading condition and consequently the same deformations. Therefore, there is no rotational constraint at the end of the flanges. As for the boundary conditions of flange plates, both end edges are simply supported except for torsional rotation, while the longitudinal edges are free in all directions.

### 3. BEHAVIOR OF A SHEAR PANEL

#### (1) Deformation

Although the behavior of model I will be extensively explained in this chapter, it should be noted that the similar observations and results have been obtained in the model II and III if not pointed out.

Fig. 3(a) shows the relationship between the load and out-of-plane displacement at the center of a web, and Fig. 3(b) depicts the configuration of out-of-plane deformations at the last step shown in Fig. 3(a). This last step will be defined as the ultimate state later on, and the load attained is called the ultimate load  $S_u$ ;  $S_p$  is the plastic shear force of web plate. Below the theoretical elastic buckling load, the rectangular panel simply deforms into a parallelogrammatic shape subjected to the elastic constraint by the flanges. Although no evident bifurcation point appears on the curve in Fig. 3(a) owing to the existence of the initial imperfection, the out-of-plane deformations of the web plate and the lateral bending or torsional deformations of the flanges start to become larger at a certain level of loading very close to this bifurcation point. Henceforth, this theoretical elastic buckling load is simply called the buckling load. As the load increases beyond this buckling load, the wavelike out-of-plane deformation induced in the diagonal area becomes larger, and becomes much more remarkable in the ultimate state. On the other hand, the bending deformations of the flanges possibly caused by the skew tensile stress in the web panel remain very small throughout the entire loading, and the flange almost holds its initial straight shape even in the ultimate state. As a result, the shape of the shear panel is still parallelogrammatic as shown in Fig. 4.

#### (2) Stress state

The stress state in the web panel is almost in pure shear before buckling. However, the tensile principal stress becomes larger in the diagonal band after buckling and the tension field begins to form. Additional loading starts yielding in the tension field, to eventually form the collapse mechanism which is defined by the full development of yielded zones to the diagonal direction. The propagation of the yielded zones is shown in Fig. 5 by the change of the number of yielded layers at several loading steps before the collapse mechanism forms. The numerals in this figure indicate the number of surfaces of the layers where the stress state is in plasticity, the maximum of which is 9. After the collapse mechanism forms, the in-plane

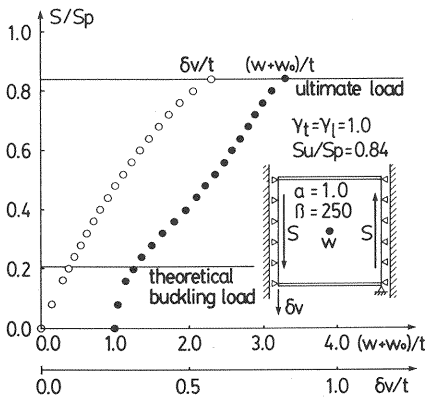


Fig. 3(a) Typical load-displacement curves of a shear panel (Model I).

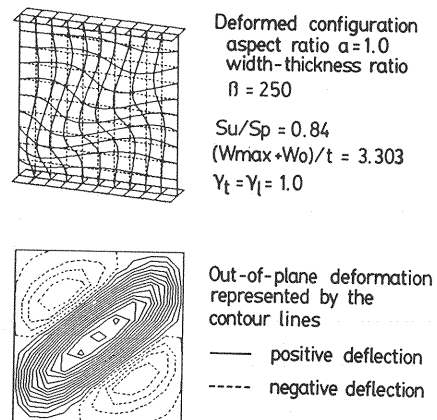


Fig. 3(b) Out-of-plane deformation in the ultimate state.

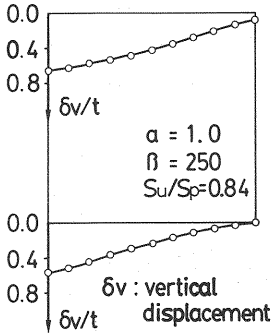


Fig.4 In-plane deformed shape of web panel (Model I; ultimate state).

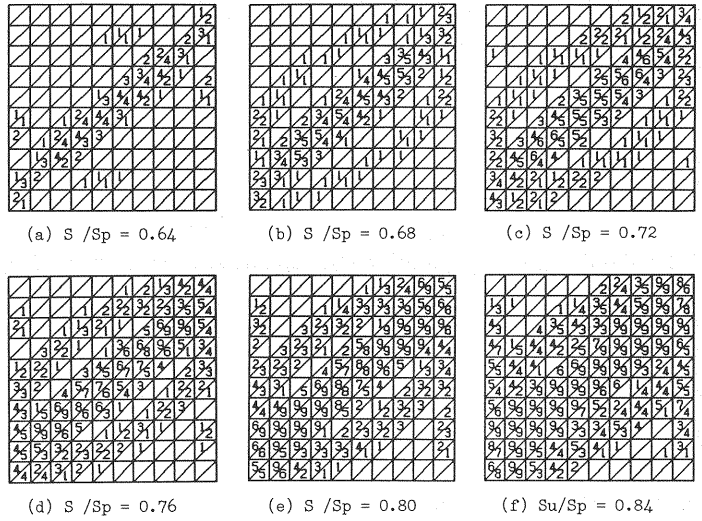


Fig.5 Development of the yielded zones (Model I,  $\alpha=1.0$ ,  $\beta=250$ ,  $\gamma=\gamma=1.0$ ).

and out-of-plane deformations of the panel become much larger, and the yielded zones spread much wider.

In this analysis, the ultimate load is defined by the load that forms the collapse mechanism, which leads to these phenomena mentioned above and finally to the significant change in the slope of the load-displacement curve as shown in Fig.6. This figure shows the load-displacement relation by the displacement-controlled analysis. The tangential line with small positive slope beyond this ultimate load is due to the effect of strain-hardening. If elastic-perfectly plastic materials are used, this slope may be decreased to zero. Hence this state in which the collapse mechanism formed is called here the mechanism state or our "ultimate state". However, the stress level of the flanges is still low enough even in this mechanism state, and no plastic hinge appears. In the same figure, the typical changes of the yielded zones in a web plate as well as flanges are also indicated. Beyond the mechanism state, the overall yielding of the web panel occurs, and the end edges of the flanges begin to yield. Although the abrupt drop of load carrying capacity is not observed, the load-displacement curve in Fig.6 has small positive slope, and so much resistance can not be expected beyond this mechanism state.

### (3) Collapse mechanism

While the boundary condition of model I expects the stiff anchor action of the tension field by the adjoining panels and makes a role of the flanges played less important than that in the actual plate girder, model II neglects the direct anchor action by the right-hand sided members and includes the relatively dominant action by the flanges. Moreover, since there exists the applied moment in model II, the bending stress plus the skew tensile stress in the tension field may bend flanges to form plastic hinges.

However, in spite of the great differences in the boundary conditions of these two models, no yielded zone develops in flanges even in the ultimate state, and no plastic hinge appears there far beyond the mechanism state. There-

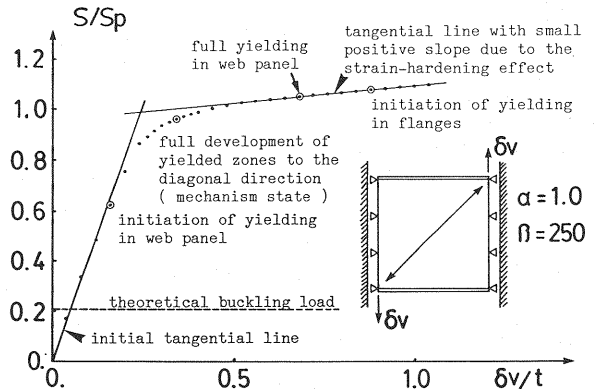


Fig.6 Development of yielded zones by the displacement-controlled analysis (Model I).

fore, our definition of the ultimate state by the formation of the collapse mechanism is quite appropriate, and the formation of plastic hinges in flanges defined as the collapse mechanism by Rockey et al.<sup>3-5</sup> can not occur in the range of structural parameters used in this analysis.

#### 4. DEVELOPMENT OF THE TENSION FIELD

##### (1) Configuration of the tension field

Fig. 7 shows the stress distribution in several cross-sections of model I whose width-thickness ratio  $\beta$  is set 250 and aspect ratio  $\alpha=1.0$  in the ultimate state. It is seen that the tensile stresses in the tension field become much larger than the compressive ones. However, the compressive stresses are also large on A'B' line near the corner region of the panel, and this effect is referred to as the gusset plate action<sup>2), 19)</sup>. Fig. 8 shows the tensile and compressive principal stresses and the angle of the tensile principal direction from the horizontal line at the center of the web P and at a typical point in its vicinity but still in the tension field band P'. As the load increases, the tensile principal stress at the midpoint P increases monotonically before yielding. After reaching the yield stress, the effective stress remains on the yield surface, but the plastic deformations progress. The final stress state is completely biaxial, and both the tensile and compressive principal stresses become the shear yield stress  $\tau_y$ , which is  $1/\sqrt{3}$  of tensile yield stress  $\sigma_y$ . At the point P', the compressive principal stresses never exceed certain values which may be achieved at buckling, while the tensile principal stresses monotonically increase beyond the yield stress level. The inclination of the tensile principal direction from the horizontal line at point P' becomes flatter with the increment of loading.

In Fig. 9, the principal stress distribution of model I in the ultimate state is shown, where the aspect ratio  $\alpha$  is 0.75, 1.0 or 1.5 but the width-thickness ratio  $\beta$  is 250. In order to demonstrate the formation of the tension field clearly, only the principal stresses whose values are larger than 80 percent of the shear yield stress are indicated in the figure. It is seen that the stress level in the diagonal area is significantly lower than that in the neighboring region. The former is in the biaxial state, while the latter is almost in the uniaxial state. This is due to the significant change of stress state on the yield surface accompanied with the development of large plastic deformation occurred in the diagonal area of the panel. The tension field looks to form a band, and the angle of its inclination is smaller than that of the diagonal line of the panel. High tensile principal stresses along the flange-side edges near the corner seem to indicate the existence of the anchor action by flanges,

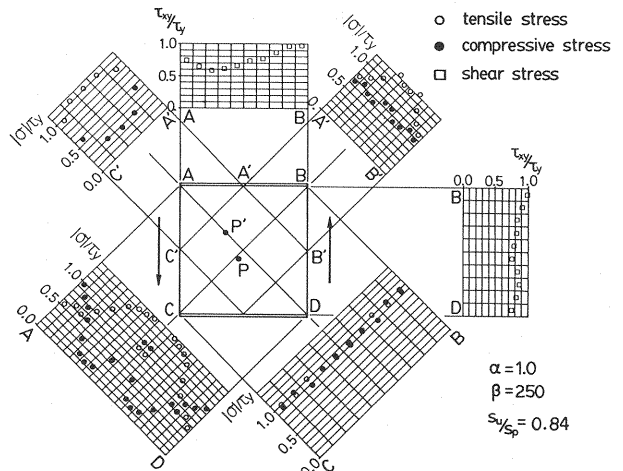


Fig. 7 Stress distribution at some cross sections in a web panel (Model I; ultimate state).

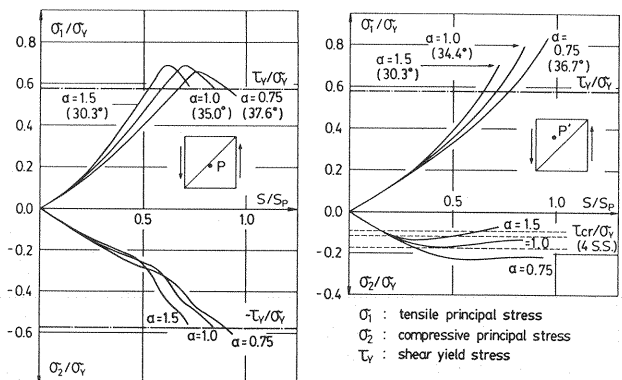


Fig. 8 Development of principal stresses at two points in the tension field (Model I).

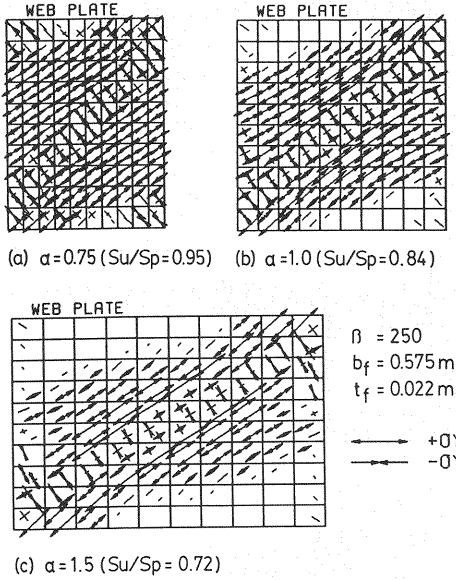


Fig.9 Tension fields of Model I.

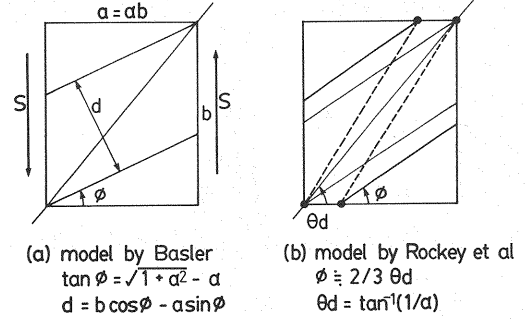


Fig.10 Typical tension field models.

and the configuration of the tension field is similar to that presented by Porter et al.<sup>4)</sup> rather than that by Basler<sup>2)</sup>. The tension fields assumed by them are shown in Fig. 10. However, the full yielding into the plate thickness direction always develops in the diagonal area of the panel. Therefore, the tension field is not always coincident with the fully yielded zones which will eventually become the cause of the collapse mechanism.

As is apparent from Fig. 9, the larger the aspect ratio becomes, the narrower the width of the tension field becomes, and the flatter the inclination of the tensile principal direction becomes. However, the tension field develops almost in the same direction of the diagonal line of the panel in the case of  $\alpha=1.5$  as in Fig. 9(c). On the other hand, if the width-thickness ratio becomes smaller, it is observed that the tension field does not develop as a band so clearly. Moreover, since the ultimate state is achieved relatively soon after buckling as shown in Table 1, the tension field does not develop so fully that the stress state is almost the same as that in the buckled state; i. e. in pure shear.

In the case of model II where the anchor action is not expected on the right-hand side edge, the stress distribution is influenced by both the shear and bending. As shown in Fig. 11, the tension field formed in the diagonal region expands even to the right-hand side edge on which the anchor action may not be expected. The compressive principal direction in this corner region is almost parallel to the edge, and no direct anchor action is recognized. The stresses become larger there and the yielding occurs. Especially, the compressive principal stress in this region becomes dominant; i. e. the gusset plate action. This large compressive principal stresses also function as an anchor of the tension field. The width at the left-hand side becomes wider than that at the right-hand side, because the applied bending stress is the largest there. On the other hand, the width at the right-hand side becomes narrower, because neither the bending stress nor the anchor action exists there. The larger the width-thickness ratio becomes, the narrower the width of the tension field becomes as has been in model I.

In the case of model III which has no flanges, the configuration of the tension field is similar to the one assumed by Basler<sup>2)</sup> of Fig. 10(a), because the direct anchor action by the flanges can not be expected at all as shown in Fig. 12. However, the tension field expands even to the upper and lower edges on which no flange is connected, and the tensile principal direction becomes almost parallel to the flanges. For larger  $\beta$ , it is also founded that the width of the tension field becomes narrower similarly to the cases of model I

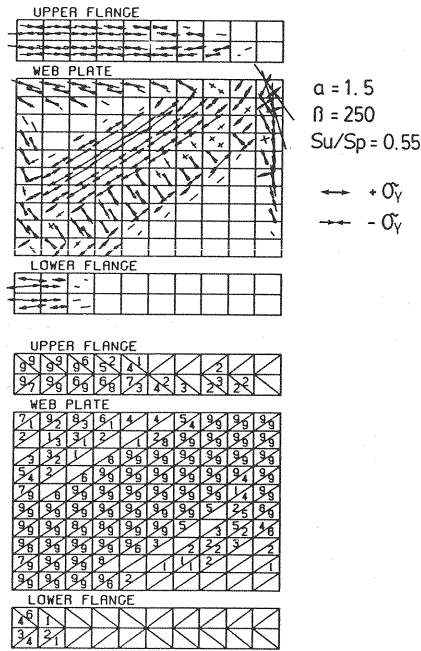


Fig. 11 Configuration of tension field and yielded zones of Model II.

and II.

(2) Direct anchor action and gusset plate action

Fig. 13 shows the tension field in the case of  $\beta=180$  and  $\alpha=1.0$ , but the flange rigidity is reduced by  $\gamma_t=\gamma_l=1/3$  and  $1/5$  from the standard one defined in the Appendix. When the flange rigidity of model I is decreased, the effect of its anchor action becomes relatively smaller to make the width of the tension field narrower, and the inclination of the tensile principal direction tends to increase, although their influence is not so significant. Moreover, in spite of the lack of anchor action in model II and III, the tension field is formed in the diagonal region and expanded even to the edges where no sided members exist. It is not the sided members but the compressive stress in the tension field that contributes to the anchor action of this field. Namely, the anchoring effect in these cases is also due to the gusset plate action.

In an actual plate girder, the tension field of each panel is anchored by the adjoining panels. Then, this continuous anchoring effect of panels makes their deformations smaller and the strength larger. Therefore, it is possible to evaluate the post-buckling behavior and the ultimate shear strength of a plate girder conservatively by the analysis of an isolated panel that does not have such continuous anchoring effect.

By the gusset plate action which acts as an anchor of the tension field without any help of the sided members and adjoining panels, both compressive and tensile principal stresses become larger in the corner

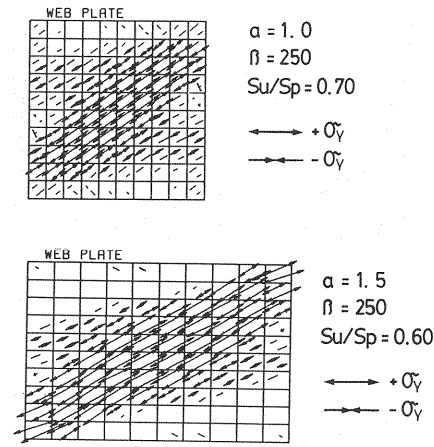


Fig. 12 Configuration of tension field of Model III.

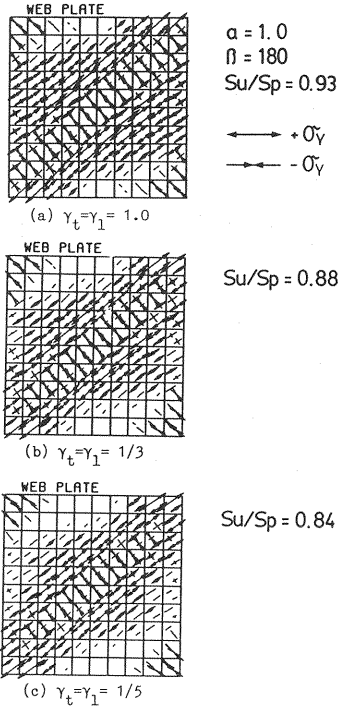


Fig. 13 Influence of the flange rigidity on the formation of tension field.



Table 1 Ultimate shear strength.

	$\alpha$	$b_f(\text{cm})$	$t_f(\text{cm})$	$\tau_{cr}/\tau_Y$	model I	model II	model III	Basler	Rockey
$\beta = 152$ $b = 152\text{cm}$ $\gamma_t = \gamma_l = 1$	0.50	44.955	1.6906	1.504	1.10	—	—	1.079	0.894
	0.75	44.955	1.6906	0.800	1.00	0.96	—	0.939	0.890
	1.00	44.955	1.6906	0.554	0.96	0.87	0.90	0.827	0.729
	1.50	44.955	1.6906	0.422	0.92	0.80	—	0.700	0.621
$\beta = 180$ $b = 180\text{cm}$ $\gamma_t = \gamma_l = 1$	0.50	48.876	1.8414	1.072	1.06	—	—	0.984	0.859
	0.75	48.876	1.8414	0.570	0.99	0.87	—	0.868	0.733
	1.00	48.876	1.8414	0.395	0.93	0.80	0.84	0.765	0.634
	1.50	48.876	1.8414	0.301	0.90	0.78	—	0.637	0.543
$\gamma_t = \gamma_l = 1/3$	1.00	37.138	1.3992	0.395	0.88	—	—	0.765	0.592
$\gamma_t = \gamma_l = 1/5$	1.00	32.685	1.2314	0.395	0.84	—	—	0.765	0.578
$\beta = 250$ $b = 250\text{cm}$ $\gamma_t = \gamma_l = 1$	0.50	57.511	2.1735	0.556	1.00	—	—	0.900	0.463
	0.75	57.511	2.1735	0.296	0.95	0.70	—	0.784	0.496
	1.00	57.511	2.1735	0.205	0.84	0.64	0.70	0.692	0.480
	1.50	57.511	2.1735	0.156	0.72	0.55	0.60	0.561	0.419
$\gamma_t = \gamma_l = 1/3$	1.00	43.699	1.6515	0.205	0.77	0.64	—	0.692	0.437
$\gamma_t = \gamma_l = 1/5$	1.00	38.460	1.4535	0.205	*	0.64	—	0.692	0.422

Remarks : the ultimate shear strength is nondimensionalized by the shear yield stress,  
 $t$  is thickness of the web plate and is set 1.0cm in all cases.  
 \* --- not converged owing to buckling.

region of the shear panel. However, in spite of the high principal stresses in this region, the initiation of yielding is not recognized. In model II, the yielded zones are produced at the left-hand side edges, but this is due to the effect of the bending stress. Therefore, the initiation of the yielded zones which develops into the collapse mechanism is not influenced directly by this gusset plate action.

## 5. CHARACTERISTICS OF THE ULTIMATE SHEAR STRENGTH

The ultimate shear strength obtained in this numerical analysis is summarized in Table 1. The theoretical elastic shear buckling strength of a web panel simply supported along its four sides and the ultimate shear strength estimated by Basler<sup>2)</sup> and Rockey et al.<sup>5)</sup> are also given in this table. Because of the boundary condition which severely restricts the deformation most by the stiffness of flanges and rigid side edges in model I, the highest strength is obtained among three models, and seems to be the upper limit of shear strength. The decrease of strength due to the reduction of the flange rigidity is not more than 10 percent even in the case when the rigidity parameters  $\gamma_t$ ,  $\gamma_l$  are set 1/5 with  $\beta=180$  and  $\alpha=1.0$ . Although the model II gives the lowest strength because of the effect of bending and the weak constraint on the right-hand side edge, it has eventually almost the same strength as the one given by Basler<sup>2)</sup>. Model III has a little higher strength than model II and gives the strength of only a web panel under pure shear loading. The comparison of the ultimate strength of model I and III might indicate that the effect of flanges is to increase the strength. The difference in the strength becomes larger as the width-thickness ratio  $\beta$  becomes larger. Model I has the strength 20 percent higher than model III in the case of  $\beta=250$  and  $\alpha=1.0$  or 1.5. In an actual plate girder, as the end shear panel is subjected to the combined loading of shear and bending and the direct anchor action by the neighboring panels and transverse stiffeners, the actual strength seems to lie in the range between those of model I and II.

## 6. CONCLUSIONS

The finite element analysis of one end shear panel isolated from a plate girder reveal the deformation behavior, the formation of the tension field and the collapse mechanism of plate girders. The observations and conclusions obtained are summarized as follows :

(1) At a certain level of loading, the fully yielded zones develop in the diagonal area in the tension field of a web plate. Since the load can not increase so much after that, this load level is defined as the ultimate load, and that phenomenon is called as the collapse mechanism.

(2) In the ultimate state, the flange plates are not bent, and no plastic hinge appears. After that state, there emerges the small yielded zone in them as observed in experiments. Therefore, the shape of a web plate in the ultimate state is parallelogrammatic. The assumption that the ultimate state is reached

when the plastic hinges form in the flange<sup>3)-5)</sup> is based on the overestimation of their direct anchor action. The yielding of the flange is not a major cause of failure of the shear panel.

(3) The collapse mechanism always develops in the diagonal direction of a web panel, while the tension field forms a band whose direction is not always coincident with that of the collapse mechanism.

(4) The tension field can form without any anchor action by flanges or sided members. In these cases, the tension field is anchored by the gusset plate action, which is the development of the high biaxial stress state in the corner end zone of the tension field. However, these high tensile and compressive stresses do not have the direct effect on the formation of the collapse mechanism.

(5) Model I shows the highest strength because of the heavy restriction and anchoring effects on the boundaries, while model II has the lowest strength owing to the effect of moment and less constraint on the right-hand side edge. Since the actual plate girder has the continuous anchoring effect by the adjoining panels, its deformation is restricted more than that of an isolated panel model. Therefore, the conservative design formula can be established by the numerical analyses of such a panel isolated from a plate girder.

## APPENDIX PARAMETERS OF FLANGE RIGIDITY

When a flange plate is modeled by a beam attached to a web plate, the effect of the flange rigidity is characterized by (1) the flexural rigidity with respect to the weak axis of the flange plate;  $E b_f t_f^3/12$ , (2) the lateral flexural rigidity with respect to the strong axis of the flange plate;  $E b_f^3 t_f/12$ , and (3) the torsional rigidity of the flange plate;  $G b_f t_f/3$ , where  $b_f$ ,  $t_f$  are the width and thickness of a flange plate respectively. As far as the cross-sectional dimensions are concerned, (1) and (3) are essentially the same parameter. In our analysis, since the flanges hold their original straight shape but are distorted after buckling of a web plate, (2) and (3) are considered as the important influence factors. In the standard design of a plate girder with the symmetric flanges, the ratio of cross-sectional area of a flange plate to that of a web is 0.5, and the width-thickness ratio of the free width of outstanding part of the flange plate is 13.0. Thus, the standard width and thickness of a flange plate  $b_{fo}$ ,  $t_{fo}$  are given as follows :

$$b_{fo} = (t + \sqrt{t^2 + 52 b t})/2, \quad t_{fo} = b t / 2 b_{fo},$$

where  $b$ ,  $t$  are the width and thickness of a web plate. The reduction of the flange rigidity from that of the standard section is represented by the following two parameters which are the reduction ratio of the torsional rigidity  $\gamma_t$  and of the lateral flexural rigidity  $\gamma_l$ ;

$$\gamma_t = b_f t_f^3 / b_{fo} t_{fo}^3, \quad \gamma_l = b_f^3 t_f / b_{fo}^3 t_{fo}.$$

Therefore, the reduced flange section is given as follows :

$$b_f = b_{fo} \sqrt[8]{\gamma_t^3 / \gamma_l}, \quad t_f = t_{fo} \sqrt[8]{\gamma_l / \gamma_t^3}.$$

## REFERENCES

- 1) Japanese Road Association : Specifications for Design of Highway Bridges, Part 2, Steel Bridges, 1980 (in Japanese).
- 2) Basler, K. : Strength of plate girders in shear, Proc. ASCE, Vol. 87, No. ST 7, pp. 151~180, 1961.
- 3) Rockey, K. C. and Skaloud, M. : The ultimate load behavior of plate girders loaded in shear, The Structural Engineer, Vol. 50, No. 1, pp. 29~47, 1972.
- 4) Porter, D. M., Rockey, K. C. and Evans, H. R. : The collapse behavior of plate girders in shear, The Structural Engineer, Vol. 53, No. 8, pp. 313~325, 1975.
- 5) Rockey, K. C., Evans, H. R. and Porter, D. M. : A design method for predicting the collapse behavior of plate girders, Proc. of the Institution of Civil Engineers, Vol. 65, Part 2, pp. 85~112, 1978.
- 6) Fujii, T. : Minimum weight design of structures based on buckling strength and plastic collapse, 3rd report, An improved theory on post-buckling strength of plate girders in shear, Journal of the Society of Naval Architects of Japan, Vol. 122, pp. 119~128, 1967.
- 7) Komatsu, S. : Ultimate strength of stiffened plate girders subjected to shear, Proc. of Colloquium of Design of Plate and Box girders for Ultimate Strength, IABSE Report, Vol. 11, pp. 49~65, 1971.
- 8) Herzog, M. A. M. : Ultimate static strength of plate girders from tests, Proc. ASCE, Vol. 100, No. ST 5, pp. 849~864, 1974.

- 9) Cescotto, S., Maquoi, R. and Massonnet, Ch. : Simulation sur ordinateur du comportement à la ruine des poutres à âme pleine cisailées ou fléchies, *Construction Metallique*, No.2, pp.27~40, 1981.
- 10) Ogihara, S. and Kuranishi, S. : An elastic-plastic analysis of web panel under shear, *Proc. of 38 th Annual Conference of JSCE*, I-97, pp.193~194, 1983 (in Japanese).
- 11) Nara, S. and Komatsu, S. : A study on the ultimate strength of steel plate under pure shear stress, *Proc. of 38 th Annual Conference of JSCE*, I-88, pp.175~176, 1983 (in Japanese).
- 12) Yoshida, Y., Amemiya, E. and Masuda, N. : A flat finite element for thin shell analysis derived by assumed stress approach, *Proc. JSCE*, No.211, pp.19~28, 1973 (in Japanese).
- 13) Yoshida, Y., Masuda, N. and Matsuda, T. : A discrete element approach to elastic-plastic large displacement analysis of thin shell structures, *Proc. JSCE*, No.288, pp.41~55, 1979 (in Japanese).
- 14) Yoshida, Y., Masuda, N., Morimoto, T. and Hirose, N. : An incremental formulation for computer analysis of space framed structures, *Proc. JSCE*, No.300, pp.21~31, 1980 (in Japanese).
- 15) Yoshida, Y., Nomura, T. and Masuda, N. : A formulation and solution procedure for post-buckling of thin-walled structures, *Computer Methods in Applied Mechanics and Engineering*, Vol.32, pp.285~309, 1982.
- 16) Yamada, Y. : Plasticity and Viscoelasticity, *The Basis and Application of Finite Element Method/Series No.6*, pp.75~111, Baifukan, Tokyo, 1980 (in Japanese).
- 17) Komatsu, S., Kitada, T. and Miyazaki, S. : Elastic-plastic analysis of compressed plate with residual stress and initial deflection, *Proc. JSCE*, No.244, pp.1~14, 1975 (in Japanese).
- 18) Moriwaki, Y. and Fujino, M. : Experimental study on shear strength of plate girders with initial imperfections, *Proc. JSCE*, No.249, pp.41~54, 1976 (in Japanese).
- 19) Niinobe, Y. : Study on the post-buckling strength of webplates of plate girders under shear, *Proc. JSCE*, No.303, pp.15~30, 1980 (in Japanese).

(Received October 27 1987)